

PACS numbers: 42.65.Hw; 42.65.Jx; 42.25.Ja; 42.55.Rz
DOI: 10.1070/QE2013v043n01ABEH014976

Small-scale instability of elliptically polarised waves in a medium with cubic nonlinearity

M.S. Kuz'mina, E.A. Khazanov

Abstract. **The boundary problem on the development of a small-scale instability of arbitrarily polarised plane waves is solved. The influence of polarisation on the spatial-perturbation gain is analysed. The maximally allowable (i.e., causing no destruction of a nonlinear medium) average intensity at a specified input noise is determined for arbitrary polarisation.**

Keywords: *small-scale self-focusing, B integral, elliptical polarisation.*

1. Introduction

The fundamental factor limiting the power of up-to-date solid-state pulsed lasers is the radiation resistance, which is determined by the concentration of defects in the bulk or on the surface of laser optical elements, induced by a high light flux. Laser systems are calculated so as to keep the radiation intensity below the destruction threshold. Due to the dependence of the refractive index on intensity, $n(I) = n_0 + \gamma_{\rm nl} I$ (n_0 is the linear refractive index and $\gamma_{\rm nl}$ is the nonlinear characteristic of the medium), self-focusing of light can be observed. The increase in the light intensity due to self-focusing may damage laser elements. In this context, self-focusing is considered as a limiting factor for the power of pulsed solid-state lasers [1 – 3].

For nanosecond solid-state lasers, the most dangerous effect is the small-scale self-focusing (SSSF) rather than the self-focusing of a beam as a whole [4, 5]. As was shown by Bespalov and Talanov [6], small-scale amplitude and phase spatial inhomogeneities, which are always present in a beam, can be amplified in a cubic nonlinear medium in the presence of a high-power wave. This leads to beam splitting into filaments, i.e., to SSSF.

It is accepted to characterise the development of self-focusing by the critical self-focusing power $P_{\rm cr}$ and the B integral (nonlinear phase shift in a medium of length L):

$$B(r) = \frac{2\pi}{\lambda}\gamma_{\rm nl}\int_0^L I(r,z)\,{\rm d}z, \qquad (1)$$

where λ is the light wavelength. At $B > 3$ the beam is split into filaments, each with a power of about $P_{\rm cr}$ [6].

Another, no less important factor, which affects significantly the development of self-focusing, is the polarisation of laser radiation. For example, when passing from linear to circular polarisation, the critical power is known to increase by a factor of 4 in media with orientational Kerr nonlinearity and by a factor of 1.5 in media with electronic Kerr nonlinearity [7]. Using circularly polarised radiation, one can increase power in the cases where it is limited by self-focusing.

The SSSF theory considers the development of harmonic small-scale perturbations with a transverse wave number $k_\perp$ in a cubic nonlinear medium against the background of an intense plane wave passing through it. This problem was solved for linearly polarised waves by Rozanov and Smirnov [8]. For arbitrarily polarised radiation, Vlasov and Talanov considered the exponentially growing solution within the linearised theory and found the boundary of the instability domain and the maximum increment [9].

The solution obtained by Vlasov and Talanov allows one to take into account the energy distribution over all spectral components of perturbation with the wave number $k_\perp$. In addition, from the practical point of view, the following two factors must be considered. First, linearly or circularly polarised radiation without a small additive of orthogonal components cannot be obtained experimentally. Second, while radiation propagates in a laser system, its polarisation may deviate from the initial, for example, due to the thermally induced birefringence in active elements [10]. Thus, it is necessary to find a complete solution to the problem of instability of arbitrarily polarised plane waves; specifically this was the purpose of our study. We obtained expressions for the main parameters characterising the change in the perturbation component when passing through a layer of nonlinear medium: the intensity gain, the polarisation ellipticity, and the angle of rotation of the polarisation ellipse. The influence of small deviation of ellipticity from zero or unity on the development of SSSF was analysed. We also estimated the maximally possible intensity (averaged over the beam cross section) for a specified noise level at the input of the nonlinear medium through which arbitrarily polarised radiation propagates.

2. Transfer matrix for elliptically polarised perturbation waves

Let us consider the propagation of arbitrarily polarised laser radiation in a medium with cubic nonlinearity. In this case, it is convenient to describe the change in the radiation parameters in terms of dimensionless complex amplitudes of right-handed (Ψ_+) and left-handed (Ψ_-) circularly polarised waves:

$$\Psi_\pm = \sqrt{\frac{c\gamma_{\rm nl}}{12\pi}}\,(E_x \pm {\rm i}E_y),$$

M.S. Kuz'mina, E.A. Khazanov Institute of Applied Physics, Russian Academy of Sciences, ul. Ul'yanova 46, 603950 Nizhni Novgorod, Russia; e-mail: kmsnn@mail.ru, khazanov@appl.sci-nnov.ru

Received 23 August 2012; revision received 22 October 2012
Kvantovaya Elektronika **43** (1) 21 – 28 (2013)
Translated by Yu.P. Sin'kov

where E_x and E_y are the transverse Cartesian components of the electric field vector and c is the speed of light in vacuum. The equations for the introduced complex amplitudes, which describe the propagation of radiation along the z axis in an isotropic medium with cubic nonlinearity, are well known [11–13]:

$$\frac{2\mathrm{i}}{k}\frac{\mathrm{d}\Psi_-}{\mathrm{d}z} = \Delta_\perp\Psi_- + \left[|\Psi_-|^2 + (1+\beta)\,|\Psi_+|^2\right]\Psi_-,$$
$$\frac{2\mathrm{i}}{k}\frac{\mathrm{d}\Psi_+}{\mathrm{d}z} = \Delta_\perp\Psi_+ + \left[|\Psi_+|^2 + (1+\beta)\,|\Psi_-|^2\right]\Psi_+, \tag{2}$$

where $k = 2\pi n_0/\lambda$, $\Delta_\perp$ is the Laplacian with respect to the transverse coordinate $r_\perp$, and the coefficient β is determined by the type of nonlinearity.

The nonlinearity due to the orientational Kerr effect plays an important role in liquids and gases. It arises in media with anisotropically polarised molecules and implies preferred orientation of the polarisation axes of molecules along the electric field. In this case, $\beta = 6$ [14]. In solids the orientational Kerr effect is close to zero, and the dominant mechanism for nanosecond (and shorter) pulses is the electronic Kerr nonlinearity. This effect is caused by deformation of electron orbitals of atoms. Here, $\beta = 1$ [14].

Vlasov and Talanov [9] investigated the stability of the solution to system (2) in the form

$$\Psi_\pm = \Psi_{0\pm}\exp\left\{-\mathrm{i}\frac{kz}{2}\left[|\Psi_{0\pm}|^2 + (1+\beta)|\Psi_{0\mp}|^2\right]\right\}, \tag{3}$$

where $\Psi_{0\pm} = \mathrm{const}$ are the complex amplitudes corresponding to an intense wave. Based on expression (3), one can easily determine the angle of rotation of the polarisation ellipse of the fundamental wave Φ_0, which is due to the field-induced anisotropy in a medium with cubic nonlinearity. This angle is equal to the half phase difference of the left- and right-handed circularly polarised radiation components: $\Phi_0 = 0.25\beta(|\Psi_{0-}|^2 - |\Psi_{0+}|^2)kz$. It was found in [9] that weak harmonic perturbations with a dimensionless transverse wave number $\kappa = \pm k_\perp/k$ are unstable in the spatial frequency band

$$0 < \kappa^2 < \kappa_{\mathrm{cr}}^2, \quad \kappa_{\mathrm{cr}}^2 = (|\Psi_{0+}|^2 + |\Psi_{0-}|^2) + \sqrt{(|\Psi_{0+}|^2 + |\Psi_{0-}|^2)^2 + 4\beta(2+\beta)\,|\Psi_{0+}\Psi_{0-}|^2}, \tag{4}$$

with the instability increment

$$h_{1,2}^2 = \frac{\kappa^2}{4}\left[\kappa^2 - (|\Psi_{0+}|^2 + |\Psi_{0-}|^2) \mp \sqrt{(|\Psi_{0+}|^2 + |\Psi_{0-}|^2)^2 + 4\beta(2+\beta)\,|\Psi_{0+}\Psi_{0-}|^2}\right]. \tag{5}$$

Analysis of expressions (4) showed that, when the fundamental-wave polarisation changes from linear ($\Psi_{0+} = \Psi_{0-}$) to circular ($\Psi_{0+} = 0$ or $\Psi_{0-} = 0$), the κ_{cr}^2 value, which determines the boundary of the instability domain, decreases by a factor of 1.5 for $\beta = 1$, provided that the intensity remains the same. Indeed, in the case of linear polarisation, the instability boundary is

$$\kappa_{\mathrm{cr\,lin}}^2 = 4\gamma_{\mathrm{nl}} I/n_0, \tag{6}$$

whereas for circular polarisation

$$\kappa_{\mathrm{cr\,circ}}^2 = {}^8\!/_3\,\gamma_{\mathrm{nl}} I/n_0. \tag{7}$$

Therefore, circularly polarised waves are spatially more stable [9].

Expression (5) allows one to find the amplitude of harmonic perturbations with a maximum increment at the output of a nonlinear element (NE) but yields no data on the amplitude of other growing perturbations. Hence, one cannot calculate the gain for a perturbation wave (noise component) with a wide perturbation spectrum. In addition, the phases and polarisations of the noise component at the NE output remain unknown. To determine these parameters, we will find the general solution to the boundary problem on the development of harmonic small-scale perturbations with a transverse wave number κ. Detailed consideration of this problem is given in the Appendix. The solution will be presented in terms of the matrix $\hat{U}$, which links the modulus $|\psi_\pm|$ and the phase φ of the complex amplitudes of left- and right-handed circularly polarised components of the perturbation wave at the input and output of a nonlinear medium of length L:

$$\begin{pmatrix} |\psi_-(L)|\begin{pmatrix}\cos\varphi(L)\\ \sin\varphi(L)\end{pmatrix} \\ |\psi_+(L)|\begin{pmatrix}\cos\varphi(L)\\ \sin\varphi(L)\end{pmatrix}\end{pmatrix} = \hat{U}\begin{pmatrix} |\psi_-(0)|\begin{pmatrix}\cos\varphi(0)\\ \sin\varphi(0)\end{pmatrix} \\ |\psi_+(0)|\begin{pmatrix}\cos\varphi(0)\\ \sin\varphi(0)\end{pmatrix}\end{pmatrix}, \tag{8}$$

Let us briefly dwell on the selected polarisation types (linear and circular), because both the fundamental wave $\Psi_{0\pm}$ and the perturbation wave, propagating in an NE, retain their polarisations. Therefore, the size of the matrix $\hat{U}$ reduces to 2×2.

The complex amplitudes of the circularly polarised perturbation components $\psi_\pm$ change equally in the case of linearly polarised fundamental wave. The expression for the matrix $\hat{U}$, which determines the change in the parameters of the perturbation component after the passage through a nonlinear medium of length L, was obtained for the first time by Rozanov and Smirnov [8]:

$$\hat{U} = \begin{pmatrix} \cosh(\eta L) & -\dfrac{k_\perp}{\sqrt{4kB/L - k_\perp^2}}\sinh(\eta L) \\ -\dfrac{\sqrt{4kB/L - k_\perp^2}}{k_\perp}\sinh(\eta L) & \cosh(\eta L)\end{pmatrix}, \quad \eta = \frac{k_\perp}{2k}\sqrt{4kB/L - k_\perp^2}\,. \tag{9}$$

In the case of right(left)-handed circularly polarised radiation, the transfer matrix $\hat{U}$ for the complex amplitudes $\psi_\pm$ takes the form

$$\hat{U} = \begin{pmatrix} \cosh(\eta L) & -\dfrac{k_\perp}{\sqrt{8kB/(3L) - k_\perp^2}}\sinh(\eta L) \\ -\dfrac{\sqrt{8kB/(3L) - k_\perp^2}}{k_\perp}\sinh(\eta L) & \cosh(\eta L)\end{pmatrix}, \quad \eta = \frac{k_\perp}{2k}\sqrt{8kB/(3L) - k_\perp^2}\,. \tag{10}$$

Formulas (9) and (10) are particular cases of the general form of matrix $\hat{U}$, the expressions for which are given in the Appendix. The waves with a polarisation corresponding to the amplitudes $\psi_\pm$ acquire a phase shift $k_\perp^2 Ln_0/(2k)$ with respect

to the fundamental wave. Expression (9) is transformed into (10) at the replacement $B \to 1.5B$. Note that this holds true only when the change in B is related to the change in intensity. If the change in B is related to the change in the NE length L (i.e., $B/L = \text{const}$), this statement does not hold true.

3. Propagation of elliptically polarised perturbation wave

3.1. Ellipticity and the angle of rotation of the polarisation ellipse

The transfer matrix $\hat{U}$ allows one to determine the ellipticity and the angle of rotation of the polarisation ellipse for a perturbation component at the NE output. These characteristics depend on the spatial frequency κ, the initial perturbation phase $\varphi(z = 0) = \varphi_0$, and the intense-wave polarisation at the NE input. Below we assume that the initial polarisation of the noise component coincides with the fundamental-wave polarisation.

The expressions for the polarisation ellipticities of the fundamental (Σ) and perturbation (σ) waves have the form

$$\Sigma = \frac{4}{\pi}\arctan\left(\frac{|\Psi_{0-}|}{|\Psi_{0+}|}\right) - 1,$$
$$\sigma(\kappa,\varphi_0,\Sigma,z) = \frac{4}{\pi}\arctan\left(\frac{|\psi_-|}{|\psi_+|}\right) - 1. \tag{11}$$

When passing from right- to left-handed circularly polarised radiation, the Σ and σ values change from –1 to +1. The characteristic changes in σ at the NE output are described in Subsection 3.3.

The angle of rotation of the polarisation ellipse of the perturbation component Φ is proportional to the phase difference of the left- and right-handed circularly polarised perturbation components:

$$\Phi(\kappa,\varphi_0,\Sigma,z) = \frac{1}{2}\left(\arctan\frac{\operatorname{Im}\psi_-}{\operatorname{Re}\psi_-} - \arctan\frac{\operatorname{Im}\psi_+}{\operatorname{Re}\psi_+}\right). \tag{12}$$

The thus introduced angle Φ does not contain the rotation of the polarisation ellipse by the angle Φ_0, which is acquired by the perturbation component along with the intense wave. Obviously, the resulting angle of rotation of the perturbation-wave polarisation ellipse is the sum of Φ and Φ_0. At large values of the B integral ($B \sim 3$), the angle Φ_0 may be as large as several tens of degrees, while the angle Φ, by which the polarisation ellipse of the noise component is additionally rotated, does not exceed 10°.

Calculations showed that the polarisation of the perturbation component at the NE output (in contrast to the NE input) does not coincide with the fundamental-wave polarisation, because we have different polarisation ellipticities ($\sigma \neq \Sigma$) and angles of rotation of the polarisation ellipse ($\Phi \neq 0$). It is convenient to describe this polarisation difference by the overlap integral

$$\chi = \frac{|\boldsymbol{E}_0(L)\,\boldsymbol{E}^*_{\text{noise}}(L)|^2}{|\boldsymbol{E}_0(L)|^2\,|\boldsymbol{E}_{\text{noise}}(L)|^2}, \tag{13}$$

which indicates what part of the perturbation wave power $\boldsymbol{E}_{\text{noise}}(L)$ at the NE output is present in the fundamental wave $\boldsymbol{E}_0(L)$. For example, in the case of linearly or circularly polarised radiation, the integral $\chi = 1$, because the polarisation of the perturbation component is retained in these cases.

3.2. Gain of the perturbation component

When radiation passes through a nonlinear medium, it is convenient to describe the change in the modulus of complex perturbation amplitudes in terms of the intensity transfer coefficient:

$$G_\pm(\kappa,\varphi_0,\Sigma,z) = \frac{|\psi_\pm(z)|^2}{|\psi_\pm(0)|^2}. \tag{14}$$

If the phase delay φ_0 of the high-power wave with respect to the perturbation wave at the input of the nonlinear medium is known, one can use (8) to obtain the gains of the right- and left-handed circularly polarised components G_+ and G_-:

$$\begin{aligned} G_+(\kappa,\varphi_0,\Sigma,z) &= [\cos\varphi_0(V_{11} + Q_{11}\tan q_0) \\ &+ \sin\varphi_0(V_{12} + Q_{12}\tan q_0)]^2 + [\cos\varphi_0(V_{21} + Q_{21}\tan q_0) \\ &+ \sin\varphi_0(V_{11} + Q_{11}\tan q_0)]^2, \\ G_-(\kappa,\varphi_0,\Sigma,z) &= \{[\cos\varphi_0(Q_{11} + U_{11}\tan q_0) \\ &+ \sin\varphi_0(Q_{12} + U_{12}\tan q_0)]^2 + [\cos\varphi_0(Q_{21} + U_{21}\tan q_0) \\ &+ \sin\varphi_0(Q_{11} + U_{11}\tan q_0)]^2\}/\tan^2 q_0, \end{aligned} \tag{15}$$

where $q_0 = (\pi/4)(\Sigma + 1)$. The expression for the gain of the perturbation component with an arbitrary polarisation ellipticity Σ has the form

$$G(\kappa,\varphi_0,\Sigma,z) = \frac{G_+ + \tan^2[(\pi/4)(\Sigma+1)]\,G_-}{1 + \tan^2[(\pi/4)(\Sigma+1)]}. \tag{16}$$

Note that the SSSF theory of Bespalov and Talanov [6] considers a partial, exponentially rising solution, for which the boundary of the instability domain is κ_{cr}. By definition, the perturbation gain beyond this region does not exceed unity. In this study we found the complete solution to the problem on the development of small-scale instability; therefore, κ_{cr} is the conditional boundary of the instability domain, and, at $\kappa^2 > \kappa^2_{\text{cr}}$, the gain G can be much larger than unity.

Using (16), one can show that the maximum noise gain G for linear and circular polarisations is determined by the B integral: $G_{\max}(\Sigma = 0) = \exp(2B)$, $G_{\max}(\Sigma = \pm 1) = \exp(^4/_3 B)$; these expressions coincide with the formulas derived in [5, 8].

Figure 1 shows the two-dimensional distribution of the total gain $G(\kappa,\varphi_0)$ for radiation with $\Sigma = 0.5$, the wavelength $\lambda = 1064$ nm, and the intensity $I_0 = 3.2$ GW cm^{-2} (averaged over the beam cross section), propagating through a layer of nonlinear medium of length $L = 33$ cm; the medium was taken to be laser neodymium glass ($\gamma_{\text{nl}} = 3.2\times10^{-7}$ cm^2 GW^{-1}). It follows from expression (16) that each set of parameters $(\kappa,\varphi_0,\Sigma)$ corresponds to a particular polarisation ellipse. Thus, the perturbation wave with initially uniform polarisation is split into differently polarised domains.

It follows also from (16) that in the $G(\kappa,\varphi_0)$ plane one can plot the curves

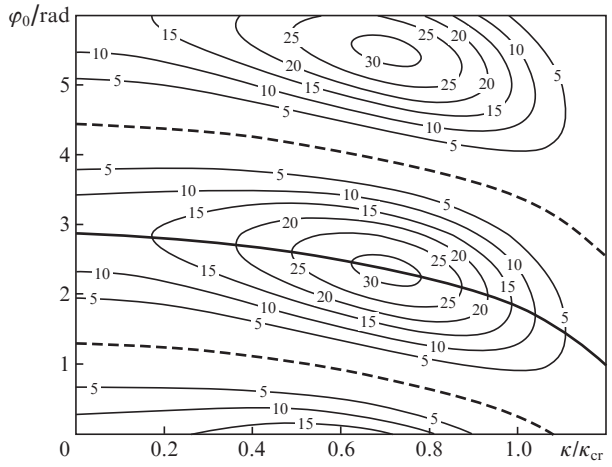

Figure 1. Two-dimensional distribution of the total gain $G(\kappa,\varphi_0)$ of the perturbation component at the output of NE of length $L = 33$ cm, made of laser neodymium glass with $\gamma_{nl} = 3.2\times10^{-7}$ cm^2 GW^{-1}, through which radiation with $\Sigma = 0.5$, $\lambda = 1064$ nm, and intensity $I_0 = 3.2$ GW cm^{-2} ($B = 2$) propagates.

$$\varphi_0^{\max}(\kappa) = \arctan\left\{\frac{\tan\varphi_+^{\max} + \tan^2[(\pi/4)(\Sigma+1)]\tan\varphi_-^{\max}}{1+\tan^2[(\pi/4)(\Sigma+1)]}\right\} + \pi m, \quad (17)$$

along which the gain is maximum, and the curves

$$\varphi_0^{\min}(\kappa) = \frac{\pi}{2} + \varphi_0^{\max}(\kappa), \quad (18)$$

along which G is minimum (here, m are integers). In Fig. 1 these curves are presented by solid and dashed bold lines, respectively. The variables $\varphi_\pm^{\max}$ in expression (17) have the same meaning as $\varphi_0^{\max}$ but for each component $\psi_\pm$ separately:

$$\begin{aligned}\varphi_+^{\max}(\kappa) = {}&{}^1\!/_2\arctan\big[2(\{Q_{11}\tan[(\pi/4)(\Sigma+1)] + V_{11}\}\\ &\times\{(Q_{12}+Q_{21})\tan[(\pi/4)(\Sigma+1)] + V_{12} + V_{21}\})\\ &\times(\{Q_{21}\tan[(\pi/4)(\Sigma+1)] + V_{21}\}^2\\ &-\{Q_{12}\tan[(\pi/4)(\Sigma+1)] + V_{12}\}^2)^{-1}\big] + \pi m,\end{aligned} \quad (19)$$

$$\begin{aligned}\varphi_-^{\max}(\kappa) = {}&{}^1\!/_2\arctan\big[2(\{U_{11}\tan[(\pi/4)(\Sigma+1)] + Q_{11}\}\\ &\times\{(U_{12}+U_{21})\tan[(\pi/4)(\Sigma+1)] + Q_{12} + Q_{21}\})\\ &\times(\{U_{21}\tan[(\pi/4)(\Sigma+1)] + Q_{21}\}^2\\ &-\{U_{12}\tan[(\pi/4)(\Sigma+1)] + Q_{12}\}^2)^{-1}\big] + \pi m.\end{aligned}$$

Note that it is not only the amplitude of the perturbation wave that changes but also the phases $\varphi_\pm$, which are determined through the elements of the transfer matrix $\hat{U}$ at the NE output:

$$\begin{aligned}\tan\varphi_+(\kappa,\varphi_0,\Sigma,z) = {}&(V_{21} + Q_{21}\tan[(\pi/4)(\Sigma+1)]\\ &+\tan\varphi_0\{V_{11} + Q_{11}\tan[(\pi/4)(\Sigma+1)]\})\\ &\times(V_{11} + Q_{11}\tan[(\pi/4)(\Sigma+1)]\\ &+\tan\varphi_0\{V_{12} + Q_{12}\tan[(\pi/4)(\Sigma+1)]\})^{-1},\end{aligned} \quad (20)$$

$$\begin{aligned}\tan\varphi_-(\kappa,\varphi_0,\Sigma,z) = {}&(Q_{21} + U_{21}\tan[(\pi/4)(\Sigma+1)]\\ &+\tan\varphi_0\{Q_{11} + U_{11}\tan[(\pi/4)(\Sigma+1)]\})\\ &\times(Q_{11} + U_{11}\tan[(\pi/4)(\Sigma+1)]\\ &+\tan\varphi_0\{Q_{12} + U_{12}\tan[(\pi/4)(\Sigma+1)]\})^{-1}.\end{aligned}$$

These expressions, in combination with (16), can be used to develop methods for suppressing SSSF in two successively located NEs, as was done in [5, 15, 16].

3.3. Integral characteristics of the perturbation component

When solving practical problems, it is important to calculate the above-introduced characteristics of the perturbation component in the entire range of instability (4) rather than at some spatial frequency κ. For correct comparison of amplification of perturbation waves with different polarisations, we will perform averaging over φ_0 and κ. Averaging over κ will be carried out in the widest range of instability $0 < \kappa^2 < \kappa_{cr\,lin}^2$, corresponding to the linear polarisation

$$\langle G(\Sigma,B)\rangle = \frac{2}{\kappa_{cr\,lin}^2}\int_0^{\kappa_{cr\,lin}}\int_0^{2\pi} G\kappa\,d\kappa\,d\varphi_0, \quad (21)$$

$$\langle\sigma(\Sigma,B)\rangle = \left(\int_0^{\kappa_{cr\,lin}}\int_0^{2\pi}\sigma G\kappa\,d\kappa\,d\varphi_0\right)\left(\int_0^{\kappa_{cr\,lin}}\int_0^{2\pi} G\kappa\,d\kappa\,d\varphi_0\right)^{-1}, \quad (22)$$

$$\langle\chi(\Sigma,B)\rangle = \left(\int_0^{\kappa_{cr\,lin}}\int_0^{2\pi}\chi G\kappa\,d\kappa\,d\varphi_0\right)\left(\int_0^{\kappa_{cr\,lin}}\int_0^{2\pi} G\kappa\,d\kappa\,d\varphi_0\right)^{-1}, \quad (23)$$

where $\kappa_{cr\,lin}$, G, σ, and χ are given by formulas (6), (16), (11), and (13), respectively. Averaging is performed on the assumption that the perturbation wave amplitude at the NE input is independent of κ; i.e., the noise component power is uniformly distributed over spatial frequencies. The dependences of $\langle G\rangle$, $\langle\sigma\rangle$, and $\langle\chi\rangle$ on the B integral and Σ are shown in Figs 2 and 3. Calculation based on formula (22) showed that, while radiation with $\Sigma \neq 0, \pm1$ propagates in an NE, the perturbation-wave ellipticity decreases in modulus; i.e., the polarisation becomes closer to linear (Fig. 2a). Thus, a small deviation (caused by the presence of orthogonal component) of the intense-wave polarisation Σ from ±1 may lead to a small increase in the self-focusing instability for waves with a polarisation close to circular.

The dependences shown in Fig. 2b suggest that the perturbation-wave polarisation varies only slightly: $\langle\chi\rangle$ decreases by no more than 0.04. The overlap integral for an initial polarisation close to linear or circular only slightly differs from unity; therefore, formulas (9) and (10) can be used in calculations.

The dependence $\langle G(\Sigma,B)\rangle$ indicates an advantage of circular polarisation in comparison with linear (Fig. 3). Let us consider this situation in more detail. Recall that the transition from linear to circular polarisation leads to narrowing of the instability band by a factor of $\sqrt{1.5}$ [see (6), (7)], and the maximum gain for circular polarisation is equal to that for linear polarisation if the replacement $B \to 1.5B$ is made. Therefore, at first glance, the solution to the problem of instability for radiation with linear polarisation and a specified B integral coincides with that for circularly polarised radiation and a B integral increased by a factor of 1.5. However, this does not always hold true, and the mean gain for a circularly

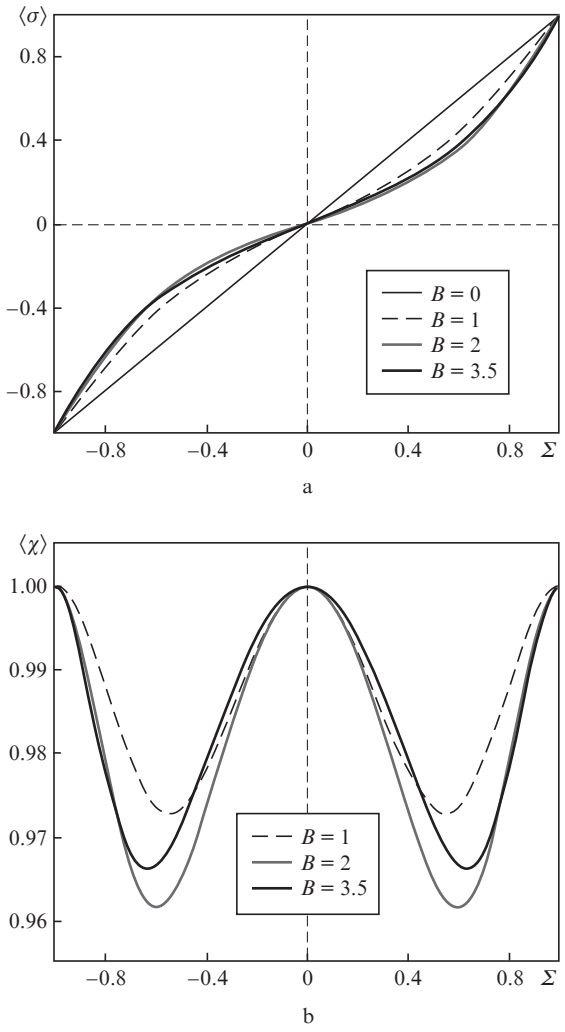

Figure 2. Dependences of the (a) polarisation ellipticity and (b) overlap integral of the perturbation wave on the ellipticity of fundamental wave polarisation at the output of a nonlinear medium of length $L = 33$ cm ($\gamma_{nl} = 3.2\times10^{-7}$ cm^2 GW^{-1}), through which radiation with $\lambda = 1064$ nm propagates, for different B values.

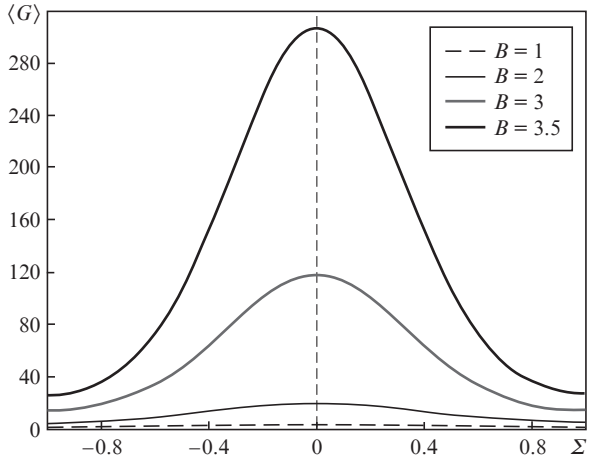

Figure 3. Dependences of the mean gain of the perturbation component on Σ in a nonlinear medium of length $L = 33$ cm ($\gamma_{nl} = 3.2\times10^{-7}$ cm^2 GW^{-1}), through which radiation with $\lambda = 1064$ nm propagates, for different B values.

polarised wave (even with a B integral increased by a factor of 1.5) can be smaller than for a linearly polarised one.

The point is that the instability boundary κ_{cr} [see (6), (7)] is determined by only the intensity, whereas the maximum gain depends on the B integral, i.e., the intensity and NE length. Below we will investigate the dependence of the gain on the intensity and NE length using the data in Fig. 4.

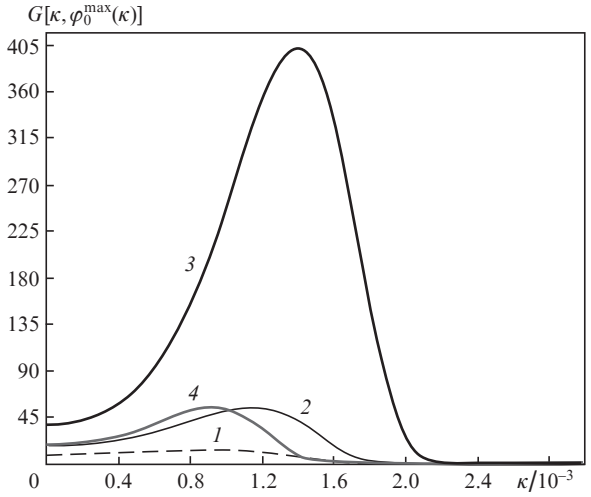

Figure 4. Functions $G[\kappa,\varphi_0^{max}(\kappa)]$ for (*1*) circular and (*2*) linear polarisations at $I_0 = 3.2$ GW cm^{-2}, $L = 33$ cm, and $B = 2$; for (*2*) circular and (*3*) linear polarisations at $I_0 = 4.8$ GW cm^{-2}, $L = 33$ cm, and $B = 3$; and (*4*) for circular polarisation at $I_0 = 3.2$ GW cm^{-2}, $L = 49.5$ cm, and $B = 3$.

The dependences $G[\kappa,\varphi_0^{max}(\kappa)]$ for linear ($B = 2$) and circular ($B = 3$) polarisations coincide [curve (*2*)], because an increase in the B integral is related to a rise in intensity. However, curve (*4*), although corresponding to the circular polarisation with $B = 3$, differs from curve (*2*): the maximum gain is 55 for both curves, but its mean is obviously smaller for curve (*4*) (i.e., for a long NE).

Let us consider the case where the B integral grows due to the increase in intensity. We will compare the mean gain of the perturbation component for linear polarisation at $B = 2$ and circular polarisation at $B = 3$. Despite the fact that curves $G[\kappa,\varphi_0^{max}(\kappa)]$ coincide in these cases, averaging according to expression (21) will be performed in different ranges of $\kappa_{cr\,lin}$ values, which are determined by the following pairs of the parameters I_0 and L: $I_0 = 3.2$ GW cm^{-2}, $L = 33$ cm and $I_0 = 4.8$ GW cm^{-2}, $L = 33$ cm, respectively. As follows from (6), the interval for the first pair of parameters is smaller than for the second pair; therefore, $\langle G(\Sigma = 0,\ B = 2)\rangle = 20$, whereas $\langle G(\Sigma = \pm1,\ B = 3)\rangle = 14.4$ (Fig. 3).

The $\langle G(\Sigma = \pm1,\ B = 3)\rangle$ value is retained for larger B values corresponding to longer NEs. Indeed, for $\Sigma = \pm1$, $I_0 = 3.2$ GW cm^{-2}, and $L = 49.5$ cm, $G[\kappa,\varphi_0^{max}(\kappa)]$ runs the same values as at $I_0 = 4.8$ GW cm^{-2} and $L = 33$ cm, but in the range of spatial frequencies narrowed by a factor of $\sqrt{1.5}$; this leads again to $\langle G(\Sigma = \pm1, B = 3)\rangle = 14.4$.

4. Limiting noise level

Small-scale amplitude spatial inhomogeneities, which are always present in a beam, are amplified against the background of intense wave. As a result, the fraction of power in

the noise component increases and, therefore, the beam-intensity modulation is amplified. Finally, this leads to optical breakdown. These effects can be minimised by controlling the noise power in the input beam, choosing appropriate polarisation, and reducing the B integral. As was indicated above, the reduction of the B integral due to the decrease in intensity is not equivalent to the reduction related to a decreased NE length. Let us formulate requirements to the intensity averaged over the beam cross section at a specified noise level at the NE input for arbitrarily polarised radiation.

Let the noise power $P_{\mathrm{n\,in}}$ at the NE input be distributed uniformly in the interval $\kappa \in [0, K]$ and set by the power spectral density $p_0 = \mathrm{const}$:

$$P_{\mathrm{n\,in}} = 2\pi \int_0^K p_0 \kappa \mathrm{d}\kappa, \tag{24}$$

$K > \kappa_{\mathrm{cr}}$ for arbitrary polarisation and any intensity. Furthermore, we assume for definiteness that $K = 3\times10^{-3}$. Then, at a $\langle G\rangle$ value much larger than unity, the noise power $P_{\mathrm{n\,out}}$ at the NE output can be estimated from the formula

$$P_{\mathrm{n\,out}} = \frac{\kappa_{\mathrm{cr\,lin}}^2}{K^2} \langle G\rangle \langle \chi\rangle P_{\mathrm{n\,in}}. \tag{25}$$

Here, the first factor is due to the following: when calculating $\langle G\rangle$ from formula (21), we integrated up to $\kappa_{\mathrm{cr\,lin}}$. The factor $\langle \chi\rangle$ indicates that we are interested in the noise power for only the polarisation coinciding with that of the fundamental wave, because the perturbation component with orthogonal polarisation does not interfere with the intense wave and, therefore, hardly contributes to the intensity modulation.

To characterise the beam inhomogeneity, some researchers use the ratio of the peak intensity to its average value, I_{peak}/I_0, [15] and some apply the ratio of rms deviation of intensity to its average value: I_{rms}/I_0 [17, 18]. The I_{peak}, I_0, and I_{rms} values are related to the fundamental-wave power P and the noise component power P_{n} by the following empirical formulas [15]:

$$I_{\mathrm{peak}}/I_0 = (1 + 5\sqrt{P_{\mathrm{n}}/P})^2, \tag{26}$$

$$I_{\mathrm{rms}}/I_0 = (1 + \sqrt{P_{\mathrm{n}}/P})^2 - 1. \tag{27}$$

The peak intensity at the NE output should not exceed the limiting value, determined by the breakdown threshold; it will be denoted as I_{th}. Using formulas (25)–(27), we arrive at a transcendental equation for the maximally allowable value (it will be denoted as I_{max}) of the average beam intensity as a function of polarisation ellipticity Σ and the fraction of the noise component power at the NE input ($P_{\mathrm{n\,in}}/P$):

$$I_{\mathrm{th}}/I_{\mathrm{max}} = \left(1 + 5\sqrt{\frac{\kappa_{\mathrm{cr\,lin}}^2}{K^2}\left\langle G(\Sigma, I_{\mathrm{max}})\right\rangle\left\langle \chi\right\rangle \frac{P_{\mathrm{n\,in}}}{P}}\right)^2, \tag{28}$$

where $\kappa_{\mathrm{cr\,lin}}$, $\langle G\rangle$, and $\langle \chi\rangle$ are determined by expressions (6), (21), and (23), respectively. Figure 5 shows the results of solution of Eqn (28) for $P_{\mathrm{n\,in}}/P = 2.2\times10^{-4}$ and 6.1×10^{-4}, i.e., according to (27) at $I_{\mathrm{rms}}/I_0 = 3\%$ and 5%, respectively.

First of all, we should note that for all curves I_{max} changes gradually from minimum for linear polarisation ($\Sigma = 0$) to maximum for circular polarisation ($\Sigma = \pm1$); the range of variation does not exceed 1.5. The reason is as follows: when I_0 increases by a factor of 1.5 and linear polarisation changes to circular, the gain $\langle G\rangle$ (and, therefore, the ratio I_{peak}/I_0) barely changes; however, the I_{peak} value increases by a factor of 1.5. For the same reason, I_{max} and B_{max} are far from proportional to I_{th}. Comparison of curves (*1′*) and (*3′*), (*1″*) and (*3″*) (Fig. 5a) shows that an increase in I_{th} by a factor of $2^1/_3$ leads to an increase in I_{max} by factors of 1.6 and 1.8 for linear and circular polarisations, respectively. The rise in I_{max} and B_{max} with a decrease in the noise level barely depends on the polarisation ellipticity Σ (the curves with single- and double-primed numbers are almost parallel).

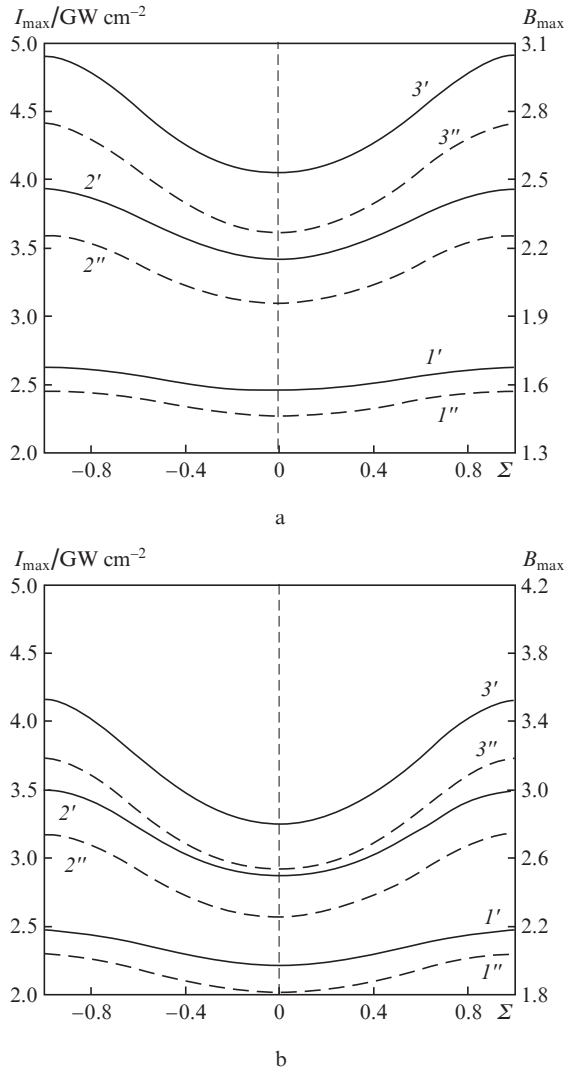

Figure 5. Dependences of the maximally possible intensity I_{max}, averaged over the beam cross section, and the value $B_{\mathrm{max}} = k\gamma_{\mathrm{nl}} I_{\mathrm{max}} L/n_0$ on the polarisation ellipticity at $I_{\mathrm{th}} = 3$ (*1′*, *1″*), 5 (*2′*, *2″*), and (*3′*, *3″*) 7 GW cm^{-2} and $I_{\mathrm{rms}}/I_0 =$ (*1′*–*3′*) 3% and (*1″*–*3″*) 5% for NEs ($\gamma_{\mathrm{nl}} = 3.2\times10^{-7}$ cm^2 GW^{-1}) with lengths $L =$ (a) 33 and (b) 49.5 cm.

It was found in [5] that a decrease in the input beam noise power by a factor of about 6 (3) makes it possible to increase the B integral by unity (half) at the same $I_{\mathrm{th}}/I_{\mathrm{max}}$ ratio. This result is confirmed by comparison of curves (*1″*) in Fig. 5a and (*1′*) in Fig. 5b. The decrease in the noise power by a factor of 3, which indicates, according to (27), a decrease in I_{rms}/I_0 from 5% to 3%, allows one to increase B_{max} approximately by half, provided that the I_{max} value is retained.

Comparison of Fig. 5a at $\Sigma = 0$ and 5b at $\Sigma = \pm1$ shows that an increase in the NE length by a factor of 1.5 and transition from linear to circular polarisation barely changes the

I_{th} value; therefore, B_{max} increases by a factor of ~1.5. This small difference is explained by the dependence of the instability boundary κ_{cr} on the intensity and polarisation type [see (6), (7)] and the dependence of the maximum gain G_{max} on the intensity, NE length, and Σ. For the aforementioned reasons, $\kappa_{cr}(\Sigma = 0) > \kappa_{cr}(\Sigma = \pm 1)$, while G_{max} and the boundary κ_{cr} coincide in the cases we are interested in. Therefore, the product $\kappa_{cr\,lin}^2\langle G(\Sigma = 0)\rangle$ is larger than $\kappa_{cr\,lin}^2\langle G(\Sigma = \pm 1)\rangle$.

Comparison of Figs 5a and 5b shows also that the use of a short NE at specified I_{th} and I_{rms}/I_0 values allows one to obtain larger I_{max} but smaller B_{max} values. From the practical point of view, it is generally important to increase intensity rather than reduce the B integral; therefore, short NEs are preferred. However, an increase in I_{max} is not proportional to decrease in the NE length. It can be seen in Fig. 5 that a reduction of the NE length by a factor of 1.5 increases I_{max} by less than 20%.

5. Conclusions

We solved the boundary problem on the development of harmonic small-scale perturbations with a transverse wave number $k_\perp$ against the background of an intense arbitrary polarisation plane wave propagating in a medium with cubic nonlinearity. Analytical expressions were obtained for the elements of the transfer matrix, which links the complex amplitudes of the perturbation component at the input and output of the nonlinear medium. The dependences of the means of the ellipticity of perturbation-wave polarisation $\langle\sigma\rangle$, the overlap integral $\langle\chi\rangle$, and the gain $\langle G\rangle$ on the fundamental-wave polarisation ellipticity Σ and the B integral were analysed.

While radiation with $\Sigma \neq 0, \pm 1$ propagates, the ellipticity of the perturbation-component polarisation decreases in modulus; i.e., the polarisation becomes closer to linear (Fig. 2a). Thus, a small deviation (due to the presence of orthogonal component) of the intense-wave polarisation Σ from ± 1 may increase the self-focusing instability for the waves with polarisation close to circular.

The polarisation of a perturbation wave during its propagation changes almost in the same way as that of the intense wave: the deviation of the overlap integral from unity at the output of a nonlinear medium does not exceed 4% (Fig. 2b). If the polarisation is close to linear or circular, the overlap integral barely differs from unity; therefore, formulas (9) and (10) can be used to calculate the gain.

The perturbation $\langle G(\Sigma, B)\rangle$ is maximum for linear polarisation and minimum for circular polarisation. It has the same value for these polarisations if the B integral for circular polarisation is larger by a factor of 1.5 (due to the increase in the length of the medium at the same intensity). However, if the B integral is increased by a factor of 1.5 due to the increase in intensity, the gain is even smaller than for linear polarisation. For example, for linear polarisation $\langle G\rangle = 20$ at $B = 2$ (Fig. 3), whereas for circular polarisation $\langle G\rangle = 14.4$ at $B = 3$.

We determined the maximally allowable (causing no destruction of NE) mean intensity I_{max} at a specified limiting intensity I_{th} and noise level for radiation with arbitrary polarisation (Fig. 5). It was shown that retainment of the I_{th}/I_{max} ratio at the same level and decrease in the noise power by a factor of 3 make it possible to increase the maximally allowable value of the B integral (B_{max}) by approximately 0.5.

An increase in the nonlinear-medium length by a factor of 1.5 and transition from linear to circular polarisation barely change I_{th}; therefore, B_{max} increases by a factor of 1.5. At the same time, in regard to the I_{max} value, the initial conditions $1.5I_0$, L, $\Sigma = \pm 1$ and I_0, $1.5L$, $\Sigma = \pm 1$ are not equivalent. At specified I_{th} and I_{rms}/I_0 values for any polarisation, larger allowable I_{max} values can be obtained in shorter NEs, while longer NEs provide larger B_{max} values.

Appendix

Having substituted the expression

$$\Psi_\pm = (\Psi_{0\pm} + \psi_\pm)\exp\left\{-\mathrm{i}\frac{kz}{2}[|\Psi_{0\pm}|^2 + (1+\beta)\,|\Psi_{0\mp}|^2]\right\},$$

($\psi_- = [A_1(z) + \mathrm{i}A_2(z)]\cos(k_\perp r_\perp)$ and $\psi_+ = [B_1(z) + \mathrm{i}B_2(z)] \times\cos(k_\perp r_\perp)$ are small perturbations) into (2), we obtain a system of differential equations for the real and imaginary parts of the complex amplitudes of perturbation waves:

$$\begin{aligned}
&\frac{2}{k}\frac{\mathrm{d}A_1}{\mathrm{d}z} = -\kappa^2 A_2,\\
&\frac{2}{k}\frac{\mathrm{d}A_2}{\mathrm{d}z} = (\kappa^2 - 2|\Psi_{0-}|^2)A_1 - 2(1+\beta)\,\Psi_{0-}\Psi_{0+}B_1,\\
&\frac{2}{k}\frac{\mathrm{d}B_1}{\mathrm{d}z} = -\kappa^2 B_2,\\
&\frac{2}{k}\frac{\mathrm{d}B_2}{\mathrm{d}z} = (\kappa^2 - 2|\Psi_{0+}|^2)B_1 - 2(1+\beta)\,\Psi_{0-}\Psi_{0+}A_1.
\end{aligned} \tag{A1}$$

The left-hand side of system (A1) contains a derivative of the column vector

$$\begin{pmatrix} A_1 \\ A_2 \\ B_1 \\ B_2 \end{pmatrix}$$

with respect to the longitudinal coordinate.

The right-hand side can be presented as a product of the 4×4 matrix $\hat{M}$, whose elements are constants, and the same column vector. In this case, the solution to (A1) can be written as a matrix exponential:

$$\begin{pmatrix}\psi_-(z)\\ \psi_+(z)\end{pmatrix} = \exp(\hat{M}z)\begin{pmatrix}\psi_-(0)\\ \psi_+(0)\end{pmatrix} = \hat{U}\begin{pmatrix}|\psi_-(0)|\begin{pmatrix}\cos\varphi_0\\ \sin\varphi_0\end{pmatrix}\\ |\psi_+(0)|\begin{pmatrix}\cos\varphi_0\\ \sin\varphi_0\end{pmatrix}\end{pmatrix},$$

where $\psi_\pm(0)$ are the perturbation amplitudes at the input of nonlinear medium; φ_0 is the initial phase of perturbation with respect to the fundamental wave; and

$$\hat{U} = \begin{pmatrix} U_{11} & U_{12} & Q_{11} & Q_{12} \\ U_{21} & U_{11} & Q_{21} & Q_{11} \\ Q_{11} & Q_{12} & V_{11} & V_{12} \\ Q_{21} & Q_{11} & V_{21} & V_{11} \end{pmatrix}$$

is the transfer matrix, whose elements have the form

$$U_{11} = \frac{\kappa^2}{4(h_1^2 - h_2^2)}\left[K_1\cosh\left(\sqrt{-h_1^2}\,kz\right) + K_2\cos(h_2 kz)\right],$$

$$U_{12} = \frac{-\mathrm{i}\kappa^2}{8h_2\sqrt{-h_1^2}\,(h_1^2 - h_2^2)} \times\left[\mathrm{i}h_2 K_4\sinh\left(\sqrt{-h_1^2}\,kz\right) + \mathrm{i}\sqrt{-h_1^2}\,K_3\sin(h_2 kz)\right],$$

$$U_{21} = \frac{-\mathrm{i}}{8h_2\sqrt{-h_1^2}\,(h_1^2 - h_2^2)}$$
$$\times\left\{b^2\kappa^2\left[\mathrm{i}h_2\sinh\left(\sqrt{-h_1^2}\,kz\right) - \mathrm{i}\sqrt{-h_1^2}\sin(h_2kz)\right]\right.$$
$$\left. + a\kappa^2\left[\mathrm{i}h_2K_1\sinh\left(\sqrt{-h_1^2}\,kz\right) + \mathrm{i}\sqrt{-h_1^2}\,K_2\sin(h_2kz)\right]\right\},$$

$$Q_{11} = \frac{b\kappa^2}{4(h_1^2 - h_2^2)}\left[\cos(h_2k_\perp z) - \cosh\left(\sqrt{-h_1^2}\,kz\right)\right],$$

$$Q_{12} = \frac{\mathrm{i}b\kappa^4}{8h_2\sqrt{-h_1^2}\,(h_1^2 - h_2^2)}$$
$$\times\left[\mathrm{i}\sqrt{-h_1^2}\sin(h_2kz) - \mathrm{i}h_2\sinh\left(\sqrt{-h_1^2}\,kz\right)\right]$$

$$Q_{21} = \frac{\mathrm{i}b}{2\sqrt{-h_1^2}\,(h_1^2 - h_2^2)}$$
$$\times\left[\mathrm{i}h_2h_1^2\sinh\left(\sqrt{-h_1^2}\,kz\right) - \mathrm{i}\sqrt{-h_1^2}\,h_2^2\sin(h_2kz)\right],$$

$$V_{11} = \frac{-\kappa^2}{4(h_1^2 - h_2^2)}\left[K_3\cosh\left(\sqrt{-h_1^2}\,kz\right) + K_4\cos(h_2kz)\right],$$

$$V_{12} = \frac{-\mathrm{i}\kappa^4}{8h_2\sqrt{-h_1^2}\,(h_1^2 - h_2^2)}$$
$$\times\left[\mathrm{i}h_2K_3\sinh\left(\sqrt{-h_1^2}\,kz\right) + \mathrm{i}\sqrt{-h_1^2}\,K_4\sin(h_2kz)\right],$$

$$V_{21} = \frac{-\mathrm{i}}{8h_2\sqrt{-h_1^2}\,(h_1^2 - h_2^2)}$$
$$\times\left\{b^2\kappa^2\left[\mathrm{i}h_2\sinh\left(\sqrt{-h_1^2}\,kz\right) - \mathrm{i}\sqrt{-h_1^2}\sin(h_2kz)\right]\right.$$
$$\left. + c\kappa^2\left[\mathrm{i}h_2K_2\sinh\left(\sqrt{-h_1^2}\,kz\right) + \mathrm{i}\sqrt{-h_1^2}\,K_1\sin(h_2kz)\right]\right\}.$$

Here, the following designations are introduced for convenience:

$$a = \kappa^2 - 2|\Psi_{0-}|^2; \quad b = 2(1+\beta)\Psi_{0+}\Psi_{0-}; \quad c = \kappa^2 - 2|\Psi_{0+}|^2;$$

$$K_1 = |\Psi_{0+}|^2 - |\Psi_{0-}|^2 - D; \quad K_2 = |\Psi_{0-}|^2 - |\Psi_{0+}|^2 - D;$$

$$K_3 = |\Psi_{0+}|^2 - |\Psi_{0-}|^2 + D; \quad K_4 = |\Psi_{0-}|^2 - |\Psi_{0+}|^2 + D;$$

$$D = \sqrt{(|\Psi_{0+}|^2 + |\Psi_{0-}|^2)^2 + 4\beta(2+\beta)\,|\Psi_{0+}\Psi_{0-}|^2}\,.$$

References

1. Potemkin A.K., Katin E.V., Kirsanov A.V., Luchinin G.A., Mal'shakov A.N., Mart'yanov M.A., Matveev A.Z., Palashov O.V., Khazanov E.A., Shaikin A.A. *Kvantovaya Elektron.*, **35** (4), 302 (2005) [*Quantum Electron.*, **35** (4), 302 (2005)].
2. Mustaev K.Sh., Serebryakov V.A., Yashin V.E. *Pis'ma Zh. Tekh. Fiz.*, **6** (14), 856 (1980).
3. Andreev A.A., Mak A.A., Yashin V.E. *Kvantovaya Elektron.*, **24** (2), 99 (1997) [*Quantum Electron.*, **27** (2), 95 (1997)].
4. Baranova N.B., Bykovskii N.E., Senatskii Yu.V., Chekalin S.V. *Tr. FIAN*, **103**, 84 (1978).
5. Poteomkin A.K., Martyanov M.A., Kochetkova M.S., Khazanov E.A. *IEEE J. Quantum Electron.*, **45** (4), 336 (2009).
6. Bespalov V.I., Talanov V.I. *Pis'ma Zh. Eksp. Tekh. Fiz.*, **3** (12), 471 (1966).
7. Zel'dovich Ya.B., Raizer Yu.P. *Pis'ma Zh. Eksp. Tekh. Fiz.*, **3** (3), 137 (1966).
8. Rozanov N.N., Smirnov V.A. *Kvantovaya Elektron.*, **7** (2), 410 (1980) [*Sov. J. Quantum Electron.*, **10** (2), 232 (1980)].
9. Vlasov S.N., Talanov V.I. *Samofokusirovka voln* (Wave Self-Focusing) (Nizhny Novgorod: Izd-vo IPF RAN, 1997).
10. Mezenov A.V., Soms L.V., Stepanov A.I. *Termooptika tverdotel'nykh lazerov* (Thermal Optics of Solid-State Lasers) (Leningrad: Mashinostroenie, 1986), p. 199.
11. Vlasov S.N., Kryzhanovskii V.P., Yashin V.E. *Kvantovaya Elektron.*, **9** (1), 14 (1982) [*Sov. J. Quantum Electron.*, **12** (1), 7 (1982)].
12. Vlasov D.V., Korobkin V.N., Serov R.V. *Kvantovaya Elektron.*, **6** (7), 1542 (1979) [*Sov. J. Quantum Electron.*, **9** (7), 904 (1979)].
13. Auric D., Labadens A. *Opt. Commun.*, **21**, 241 (1977).
14. Fibich G., Ilan B. *Phys. Rev. E*, 036622 (2003).
15. Garanin S.G., Epatko I.V., L'vov L.V., Serov R.V., Sukharev S.A. *Kvantovaya Elektron.*, **37** (12), 1159 (2007) [*Quantum Electron.*, **37** (12), 1159 (2007)].
16. Vlasov S.N., Yashin V.E. *Kvantovaya Elektron.*, **8** (3), 510 (1981) [*Sov. J. Quantum Electron.*, **11** (3), 313 (1981)].
17. Williams W.H., Auerbach J.M., et al. *Proc. SPIE Int. Soc. Opt. Eng.*, **3264**, 93 (1998).
18. Wegner P. et al. *LLNL. ICF Quarterly Report UCRL-LR-105821-99-1* (Livermore, Cal, 1996).